

High-Spin State Dynamics and Quintet-Mediated Emission in Intramolecular Singlet Fission

Jeannine Grüne^{1,2,*}, Steph Montanaro³, Thomas W. Bradbury⁴, Ashish Sharma¹, Simon Dowland¹, Sebastian Gorgon¹, Oliver Millington³, William K. Myers², Jan Behrends⁵, Jenny Clark⁴, Akshay Rao¹, Hugo Bronstein^{1,3}, Neil C. Greenham^{1,*}

¹*Cavendish Laboratory, University of Cambridge, Cambridge CB3 0HE, U.K.*

²*Centre for Advanced Electron Spin Resonance, University of Oxford, Oxford OX1 3QR, U.K.*

³*Department of Chemistry, University of Cambridge, Cambridge CB2 1EW, U.K.*

⁴*Department of Physics and Astronomy, University of Sheffield, Sheffield S3 7RH, U.K.*

⁵*Fachbereich Physik, Freie Universität Berlin, 14195 Berlin, Germany.*

*Corresponding authors. Email addresses: jg2082@cam.ac.uk (Jeannine Grüne), ncg11@cam.ac.uk (Neil C. Greenham)

Abstract

High-spin states in molecular systems hold significant interest for a wide range of applications ranging from optoelectronics to quantum information and singlet fission (SF). Quintet and triplet states play crucial roles, particularly in SF systems, necessitating a precise monitoring and control of their spin dynamics. Spin states in intramolecular SF (iSF) are of particular interest, but tuning these systems to control triplet multiplication pathways has not been extensively studied. Additionally, whilst studies in this context focus on participation of triplet pathways leading to photoluminescence, emission pathways via quintet states remain largely unexplored. Here, we employ a set of unique spin-sensitive techniques to investigate high-spin state formation and emission in dimers and trimers comprising multiple diphenylhexatriene (DPH) units. We demonstrate the formation of pure quintet states in all these oligomers, with optical emission via quintet states dominating delayed fluorescence up to room temperature. For triplet formation, we distinguish between SF and ISC pathways, identifying the trimer Me-(DPH)₃ as the only oligomer exhibiting exclusively the desired SF pathways. Conversely, linear (DPH)₃ and (DPH)₂ show additional or exclusive triplet pathways via ISC. Our comprehensive analysis provides a detailed investigation into high-spin state formation, control, and emission in intramolecular singlet fission systems.

Introduction

Molecular high-spin states present a diverse platform for organic optoelectronics that involve complex processes requiring transition between different spin states.¹⁻⁴ One key application is singlet fission (SF), a fast, spin-conserving photophysical process converting singlet excitons rapidly into spin-correlated triplet pairs, before these dissociate into free triplets.^{1,5} This principle has a significant potential impact on enhancing photovoltaic efficiency as photocurrent generation occurs from each triplet state.^{6,7} Additionally, the formation of quintet states emerges as a critical aspect of the fission process, offering potential applications beyond photovoltaics, such as in quantum computing and spintronics.^{8,9}

Whilst intermolecular SF has been extensively studied, we focus on intramolecular singlet fission (iSF), where molecular structures can be tuned to control the rates and generation of triplet pairs.¹⁰⁻¹⁵ Recent literature have primarily explored iSF in dimers, for instance pentacene^{16,17} and tetracene¹⁸⁻²⁰ dimers, with only a few trimer studies that differ in SF process.^{21,22} A key question to answer is whether additional units facilitate spatial separation of triplet excitons, reducing the likelihood of competing, efficiency-reducing, intersystem crossing (ISC). Furthermore, studies have shown the importance of not only the singlet and triplet states but also the quintet states that form during this process; for instance in crystals, dimers and MOFs.^{8,9,14} Although the formation of quintet states has been investigated, the quintet back pathway leading to photoluminescence has not been addressed.

Here, we seek to understand the molecular design principles that favour the formation of quintets and free triplets in oligomer systems. Our previous work reported the synthesis of oligomers based on diphenylhexatriene (DPH) units, demonstrating with optical characterization the ability of forming triplet states.²³ However, the role of high spin states, i.e. the precise formation pathway of triplet states and the involvement of the quintet states, remained an open question. We discern the underexplored participation of quintet states in emission and the formation of triplets via SF or via the less-efficient pathway of ISC. Upon tuning trimer configurations by adding methyl groups, we further investigate the effect of planarity on high spin states generation.²⁴ Our goal is to identify molecules that can effectively form triplets through SF and emit via quintet states, thus optimizing materials for both energy conversion and quantum computing applications.

We address these questions with unique set of advanced spin-sensitive measurements that allow us to distinctly track the formation and emission pathways of spin states with different multiplicities. Electron paramagnetic resonance (EPR) is particularly powerful for detecting the formation and dynamics of both triplet and quintet states, providing critical insights into the pathway of SF.^{5,14} Optically detected magnetic resonance (ODMR) offers a complementary approach for the optical readout of spin states, enabling precise measurement of spin states participating in PL, even up to room temperature. Transient magnetic field effect (MFE) studies further confirm the nature of intermediate triplet pair states, giving a comprehensive picture of the spin dynamics in iSF.²⁵ This set of measurement techniques is unique for studying high spin states in iSF and enables us to track the formation and emission pathways of quintet and triplet states in a precise manner.

We especially focus on the methylated trimer Me-(DPH)₃, in comparison with the linear arranged trimer (DPH)₃ and dimer (DPH)₂, to elucidate their quintet and triplet state formation and emission back pathway. Our study shows that quintet states dominates delayed emission across all three materials, even at room temperature. We are able to distinguish between triplets generated by SF and ISC at various temperatures and molecular geometries and develop a kinetic model for their dynamics. Our findings reveal that quintets are consistently produced in all oligomers, with the methylated trimer particularly efficient in suppressing ISC and favouring SF-generated triplets. This comparative analysis provides a general framework for designing DPH oligomers suitable for both quintet generation for quantum computing applications and exciton multiplication for energy-related applications.

Long-lived high-spin states in DPH oligomers

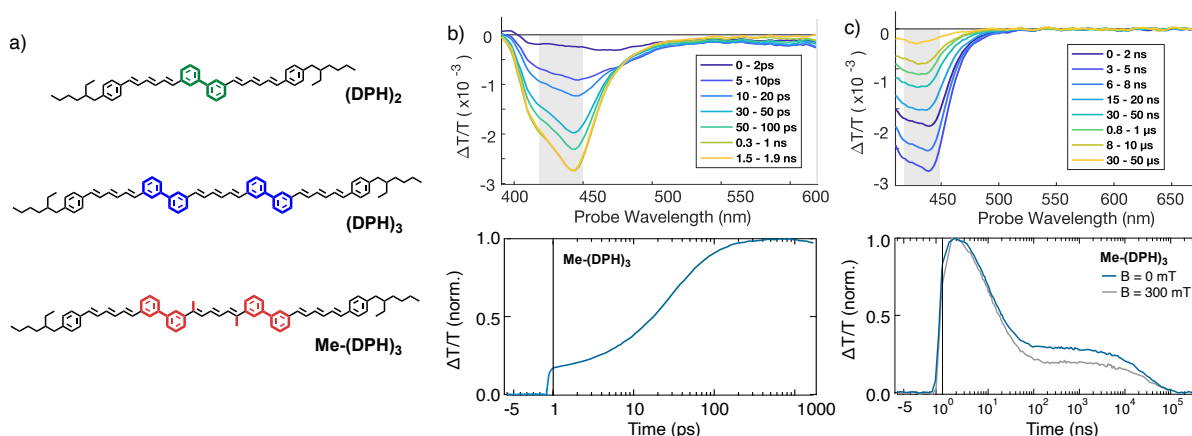


Fig. 1. Molecular structure of all oligomers and TA of methylated DPH trimer Me-(DPH)₃. a) Molecular structures of linear DPH dimer (DPH)₂, trimer (DPH)₃, and methylated trimer Me-(DPH)₃. b) TA spectra (top) and kinetics (bottom) of Me-(DPH)₃ in the picosecond regime revealing fast formation of ⁿ(TT) states. c) TA spectra (top) and kinetics (bottom) of Me-(DPH)₃ in the nanosecond regime revealing decay of ⁿ(TT) and long living T₁ states.

Fig. 1a illustrates the molecular structure of the DPH oligomers investigated. As previously reported, (DPH)₂ and (DPH)₃ consist of two or three directly connected DPH chromophores, with terminal 2'-ethylhexyl groups (DEH) to aid solubility. The newly introduced Me-(DPH)₃ is distinguished by the inner unit being replaced by 1,6-dimethyl-diphenylhexatriene to study the impact of methyl substituents, as previously used in monomers and already established in carotenoids (for further synthetic details, see Supporting Information).^{1,26,27}

To demonstrate the rapid formation of triplet pairs (TT), Fig. 1b shows picosecond transient absorption (TA) spectroscopy on Me-(DPH)₃. Upon excitation with a 400 nm pump pulse of 200 fs duration, a broad photoinduced absorption (PIA) is immediately observed, which diminishes, concomitant with the growth of an intense higher energy PIA within a few tens of picoseconds. The initial PIA is typically associated with S* transitions, with S* being denoted as the singlet state in DPH literature, based on rapidly equilibration of the S₁ and S₂ states on sub-picosecond timescales.²⁸ The rapid emergence of the higher energy PIA is ascribed to the fast generation of strongly-correlated triplet pair states with singlet character, which we refer to as ¹TT.^{29,30} Nanosecond TA (Fig. 1c) initially reveals the decay of the TT state in an exponential decay with $\tau = 12$ ns, followed by the appearance of a long-lived plateau. Based on magnetic field-dependent TA, and measurements discussed below, we attribute the initial magnetic-field independent decay to TT states, and the magnetic-field dependent plateau to high-spin states generated via SF.

Probing High-Spin State Formation by Electron Paramagnetic Resonance

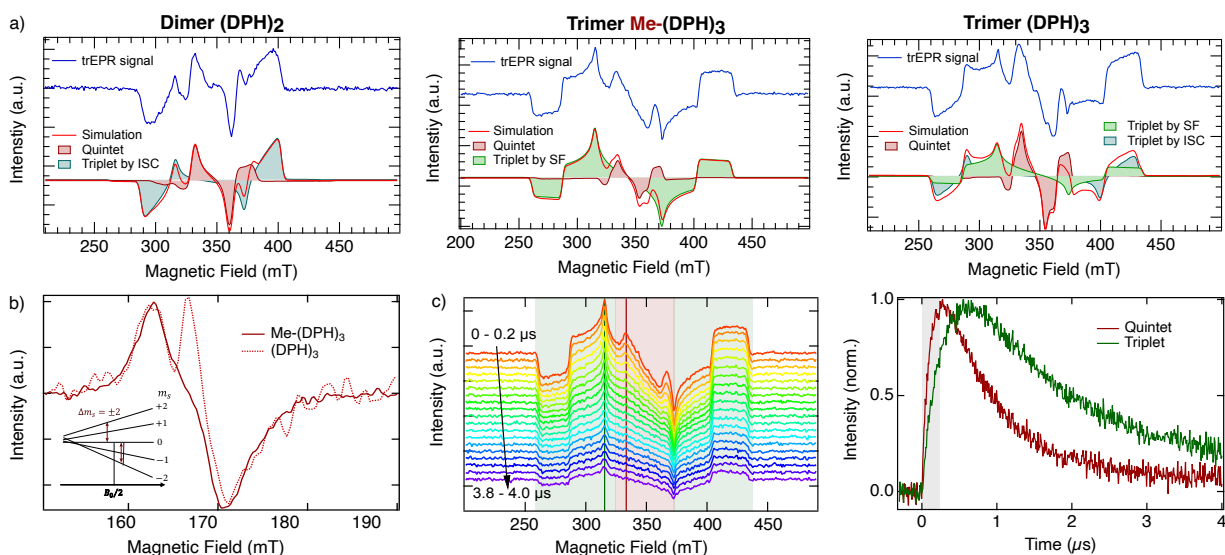


Fig. 2. Electron paramagnetic resonance to probe quintet and triplet generation. a) TrEPR spectra (blue) and simulation (red) from 0 – 500 ns for $(DPH)_2$, Me- $(DPH)_3$ and $(DPH)_3$. Me- $(DPH)_3$ reveals quintet (red filled) and triplet (green filled) formation via singlet fission process, whilst $(DPH)_2$ and $(DPH)_3$ show triplet formation only or additionally via ISC (blue filled). b) Half-field (HF) signal ($\Delta m_s = 2$ transitions) reveal only quintet features for Me- $(DPH)_3$ whilst $(DPH)_3$ additionally exhibit HF signal from ISC triplets. c) TrEPR spectra for Me- $(DPH)_3$ exhibit faster decay of quintet signal and long-lived triplet states. Time slices for the quintet ($B = 335$ mT) and triplet ($B = 305$ mT) show different peak times and decay behaviour (response time marked in grey). Measurements performed at $\lambda = 355$ nm and $T = 80$ K.

To investigate the formation of triplet states and higher spin multiplicity pair states, we performed trEPR measurements. Fig. 2a presents the trEPR spectra of $(DPH)_2$, Me- $(DPH)_3$, and $(DPH)_3$ for 0 – 500 ns (blue). All spectra exhibit multiple transitions, indicating non-thermalized high-spin states. Common features in all spectra include absorptive/emissive transitions at 330 mT and 360 mT, respectively, with variations in outer transitions. Simulations (red, EasySpin³¹ parameters Table S1) and pulsed EPR measurements (Fig. S2) identify the inner transitions as the $m_s = 0 \rightarrow \pm 1$ transition of the strongly correlated triplet pair 5TT , representing a pure quintet state with $S = 2$.^{5,14} The zero-field splitting parameters $D_Q = 750$ MHz and $E_Q = 80$ MHz are consistent with the expected splitting of $D_T/3$ ($D_T = 2450$ MHz as shown later) for a coupled triplet pair 5TT in the strong exchange limit.^{5,32} This correlation indicates that, although the quintet state forms through singlet-quintet mixed states of weakly-spin correlated triplet pairs (SCTPs), it ultimately transitions to a longer-lived pure quintet state within the strongly-coupled regime.

Whilst quintet state formation is verified in all three oligomers, triplet state formation differs, as represented in the additional outer transitions. If the weakly Sctp does not re-form into a

strongly-coupled state, it can dissociate, resulting in a further reduction in J and the formation of free or very weakly-coupled triplet excitons. They inherit the same spin polarization as the SCTP with selective $m_s = 0$ level population, resulting in an *eaaeaa* pattern (with microwave emission (*e*) and absorption (*a*) in the three canonical orientations). Reviewing Me-(DPH)₃, the outer transitions (green filled) can be attributed to this pathway, evidenced by its selective $m_s = 0$ population. The ZFS parameters $D_T = 2450$ MHz and $E_T = 270$ MHz align with the DEH-DPH monomers, suggesting the SF-derived triplet states form on the outer chromophores (Fig. S3).

In contrast, the triplet features in (DPH)₂ and (DPH)₃ cannot be solely reproduced by SF polarization. Instead, formation of triplets in (DPH)₂ can be attributed to ISC, leading to a population of the zero-field sublevels of $[p_x, p_y, p_z] = [0 \ 1.00 \ 0.52]$ with $D_T = 2450$ MHz. DEH-DPH monomers in dilute toluene solution, that can only undergo ISC, reveal the same pattern in trEPR (Fig. S3) and confirm the ISC pathway. Whilst (DPH)₂ can still form pure quintet states via singlet-quintet mixing in the weakly SCTP, its inability to efficiently reduce J with two chromophores leads to triplet formation solely by ISC. We exclude the possibility of these triplets being ³TT states based on ODMR results discussed later.

Strikingly, (DPH)₃ exhibits a distinct spectral shape that does not correspond to SF or ISC mechanisms alone. However, by combining the simulation from Me-(DPH)₃ with the ISC pattern from (DPH)₂, the spectra can be accurately reproduced. While the SF-generated triplets in (Me)-(DPH)₃, the ISC-generated triplet in (DPH)₂, and the monomer exhibit a D_T value of 2450 MHz, the ISC-generated triplet in (DPH)₃ shows an increased $D_{T,ISC}$ value of 3500 MHz with $[p_x, p_y, p_z] = [0 \ 1.00 \ 0.52]$, indicating an increased localization within the trimer given the more complex energetic landscape.³³

To selectively probe the quintet state, we measured the $\Delta m_s = 2$ transitions at half the resonant magnetic field B_0 , known as the half-field (HF) signal (Fig. 2b).³⁴ Me-(DPH)₃ exhibits a derivative-shaped HF signal with both absorption and emission features, which can only stem from a quintet state with multiple possible $\Delta m_s = 2$ transitions (see inset). Examining (DPH)₃, we observe the same HF signal as the quintet state, along with an additional triplet HF signal. In contrast to SF-generated triplet states with selective $m_s = 0$ population, ISC-derived triplets

in (DPH)₃ have sufficient spin polarization between $m_s = \pm 1$ and confirms the observation from the trEPR spectra in full-field.

To better understand temporal spin state formation, we examined the time evolution of the EPR signal. Fig. 2c displays the trEPR spectra for Me-(DPH)₃ in 200 ns intervals up to 4 μ s. Initially, the quintet signal (red) dominates, peaking within the instrument response time (≈ 100 ns, grey) and decays with a time constant of ~ 2 μ s. In contrast, the triplet signal (green) peaks later at ~ 800 ns, and displays a more prolonged decay. The faster decay of the quintet state is attributed to a pathway leading to measurable PL and providing optical readout, which will be discussed below.

Revealing quintet-mediated emission by spin-sensitive PL

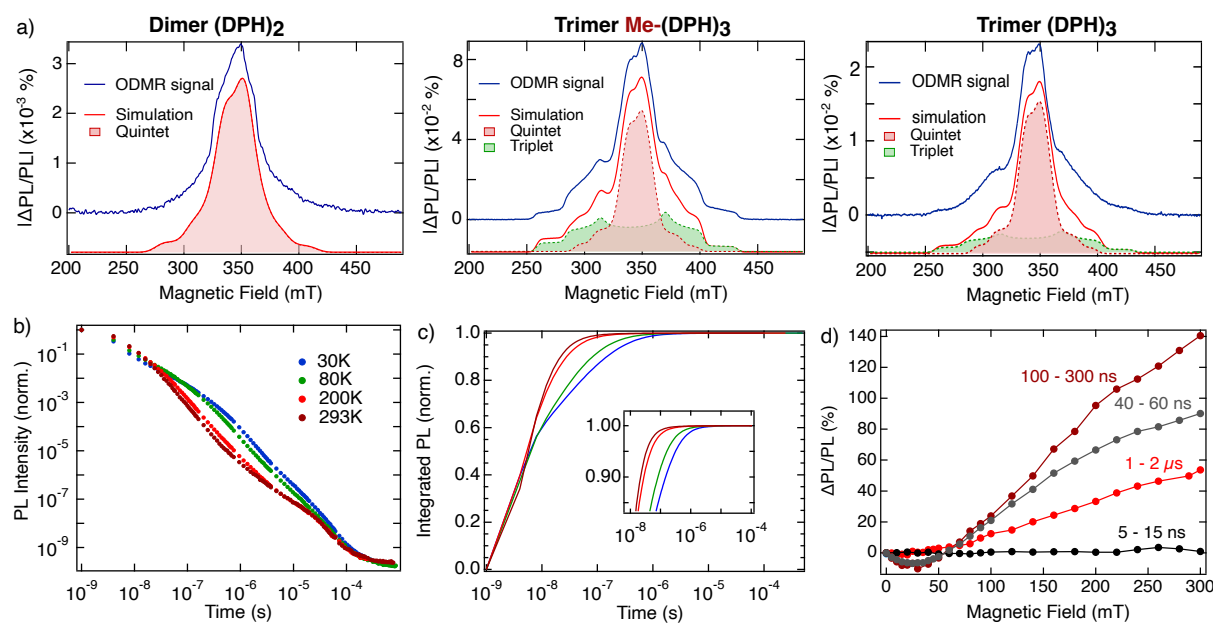


Fig. 3. Spin-dependent luminescence. a) ODMR spectra (blue) and simulation (red) for (DPH)₂, Me-(DPH)₃, and (DPH)₃. Whilst the trimers show involvement of both quintet (red filled) and triplet (green filled) in the luminescence, the dimer only reveals quintets. Performed at $T = 80$ K and $\lambda = 365$ nm. b) Temperature dependent PL of Me-(DPH)₃, exhibiting long time delayed fluorescence. c) Integrated PL from (b), revealing most of the luminescence decayed by 1 μ s. d) Time-dependent magnetic-field dependent PL of Me-(DPH)₃. The spin-dependent luminescence starts at 40 ns, with reaching a maximum at 100-300 ns. 200 μ M in toluene for solutions, 0.1 wt% in polystyrene for films. Performed at $\lambda = 375$ nm and $T = 80$ K (temperature dependence in Fig. S9).

Whilst EPR shows the possibility of manipulation of the high-spin states, readout can be performed by optical techniques, such as optically detected magnetic resonance (ODMR).^{9,35} ODMR employs the principles of EPR by using microwave irradiation to alter the spin

polarization between sublevels. Under continuous illumination, simulating realistic conditions, the PL readout changes as the sublevel population varies under magnetic resonance.³⁶

Fig. 3a presents the ODMR spectra for the dimer (DPH)₂ and both trimers, Me-(DPH)₃ and (DPH)₃ at $T = 80$ K whilst the temperature dependence from 10 K to 293 K is discussed further below. The dimer displays only the response of the quintet state, whilst the ISC triplet does not participate in the PL, proving an optical pathway from the quintet state to the emissive singlet state. The quintet state is also visible in both trimers, Me-(DPH)₃ and (DPH)₃, with the SF-generated triplet being visible as well at $T = 80$ K. The spectral features are consistent with the EPR simulation in Fig. 2, confirming the involvement of quintet and triplet states. Since the dimer shows only quintet involvement, the triplet feature in the trimers likely does not correspond to ISC to ³TT, as that state would also be accessible in the dimer. The pronounced HF signal (Fig. S4) additionally confirms the involvement of the quintet state.

The temperature-dependent trPL of Me-(DPH)₃ (Fig. 4b) shows a persistence of delayed PL for up to hundreds of nanoseconds, confirming the participation of high-spin states. Whilst maintaining the same PL spectrum with time and temperature (Fig. S5, S6), a multicomponent decay is observed, with slowed-down dynamics when lowering the temperature. Integrated PL (Fig. 4c) shows that 99.99% of the emission occurs within 2 μ s at all temperatures; with higher temperatures reaching this threshold faster. EPR data presented earlier revealed quintet states decaying within 2 μ s, consistent with negligible PL after the same time, suggesting that quintet states predominantly contribute to PL. ODMR results at room temperature (see below) confirm the dominance of quintet emission under ambient conditions.

Furthermore, all three oligomers, including (DPH)₂ with only ISC-generated triplets, show a comparable trPL decay (Fig. S7). The equivalent generation of quintet states in all oligomers supports the quintet state being the major reservoir of delayed fluorescence.

The nature of the intermediate triplet pair states in Me-(DPH)₃ can be further probed via PL under applied magnetic field (Fig. 4d). The MFE and the underlying mechanisms in DPH crystals and films have been extensively explored in previous studies.³⁷⁻³⁹ The zero-crossing typically seen at 50 mT in Me-(DPH)₃ is comparable to DEH-DPH films (Fig. S8), with both exhibiting the same zero-field splitting value D .⁴⁰ However, whilst the overall MFE shape in Me-(DPH)₃ is similar to the previously reported MFE in DPH, variations lie in the time dependence. The initial 15 ns show no magnetic field dependence, followed by emerging effects at \sim 30-40 ns. This agrees with the magnetic-field-independent decay of nsTA (Fig. 1c),

indicative of initially strongly-coupled triplet pairs contributing to PL. After 40 ns, the system enters the weakly SCTP regime, resulting in a MFE contrast of up to 140% within 100-300 ns. Notably, the MFE response diminishes significantly at 1-2 μ s, at later times becoming nearly undetectable (Fig. S9). No evidence of triplet-triplet annihilation (TTA) from free triplets, which would manifest as a reverse SF profile, was observed at any time, indicating a minor contribution of free triplets to PL.⁴¹

Temperature-Dependence of Quintet and Triplet Dynamics

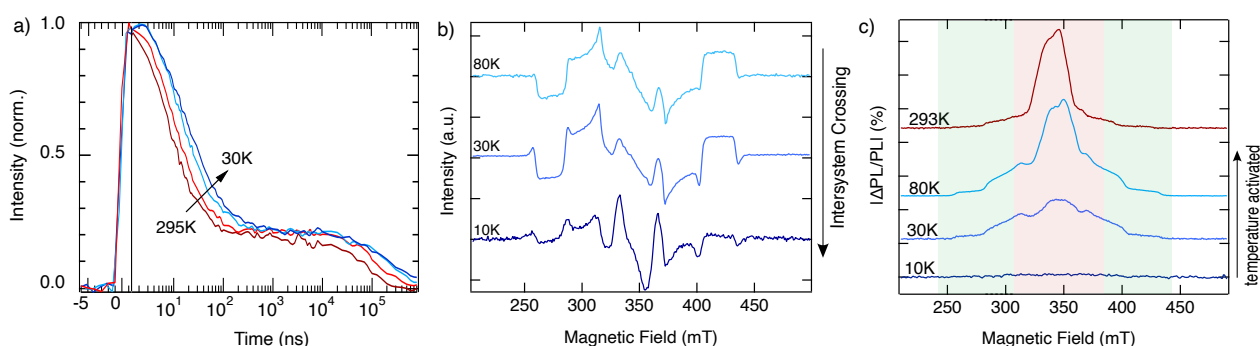


Fig. 4. Temperature dependence of Me-(DPH)₃. a) TA kinetics in nanosecond regime, exhibiting faster decay with increasing temperature, but long-lived triplets for all temperatures. b) Temperature-dependent trEPR spectra (0 - 500 ns). Quintet and triplet formation is present at all temperatures, whilst the ISC contribution increases with decreasing temperature. c) Temperature-dependent ODMR spectra. Whilst at 80 K the data show involvement of quintet (red) and triplet (green) states in the PL, the ratio decreases and no high spin states are visible at 10 K.

To assess the energetics and temperature dependence of quintet and triplet formation, we conducted temperature-dependent measurements. Figs 4a and 4b present the temperature-dependent TA and EPR analyses of quintet and triplet state formation, while PL measurements (ODMR, Fig. 4c) illustrate the temperature dependence of optical readout.

Fig. 4a demonstrates a temperature-dependent decay rate of the initial TA signal, attributed to ¹TT states. This faster decay with higher temperatures is consistent with the trPL data (Fig. 3a) and implies overall faster (non-)radiative pathways to the ground state.⁴² However, the plateau height remains almost temperature-independent. As known from carotenoids, some molecular conformation might undergo a (temperature-dependent) decay to the ground states, whilst some other conformations undergo SF.²⁶ The temperature-independent SF formation aligns with the temperature-dependent trEPR (Fig. 4b), where quintet and triplet formation are evidenced for all temperatures down to 10K, with similar quintet-triplet ratio from 30K. We showed that at 80K (Fig. 2a) quintets and triplets are only generated via SF in Me-(DPH)₃. However, lowering

the temperature induces triplets generated by ISC, resulting in spectral features that resemble those of unmethylated (DPH)₃. It has previously been well established in carotenoids that methyl groups perturb the planarity of the conjugated region²⁷ as well as undergo internal rotations that are still present in frozen toluene.^{43,44} However, it is observed that temperatures below 80 K freeze out the methyl group rotations, hindering possible terahertz motions supporting SCTP formation, and increasing the proportion of ISC.^{45,46}

The optical back-pathway shows a more dominant temperature activation, displayed in temperature-dependent ODMR (Fig. 4c). The quintet/triplet ratio decreases towards 30 K, whilst no high-spin states are visible at 10 K. However, high-spin formation was evidenced at 10 K in trEPR, indicating a temperature activation to the emissive state. The quintet shows a higher temperature activation until 80 K, suggesting the necessity to overcome an additional temperature barrier by exchange interaction. Importantly for quintet states in spintronic applications, we predominantly observe quintet state emission even at 293 K in ODMR, indicating long-lived quintet states with preserved spin polarization at room temperature.

Discussion

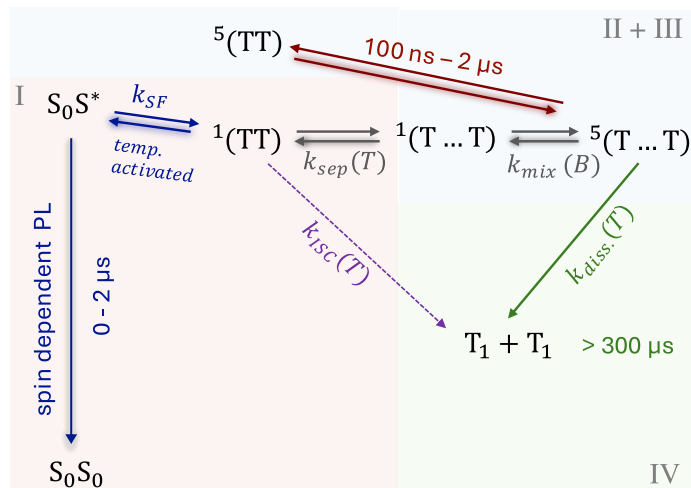


Fig. 5. Overview of generation pathways for quintet and triplet states as well as optical back-pathway. The singlet fission process generates $1TT$ states (Regime I) that can separate into weakly-coupled triplet pair states (Regime II, III). These can, after magnetic-field dependent mixing, either be back-transferred to strongly-coupled $5TT$ states that have an optical readout pathway (Regime III) or dissociate into free triplets (Regime IV).

Based on the unique set of spin-sensitive measurements performed, we construct a comprehensive understanding of the photophysical processes in DPH oligomers, particularly focusing on quintet and triplet states. Fig. 5 illustrates the formation pathway and the optical

back-pathway of quintet and triplet states in Me-(DPH)₃, which we can temporally divide into four distinct regimes:

1. **Regime I (0 - 40 ns):** This regime is characterized by the presence of strongly-coupled triplet pairs. We observe a temperature-dependent (Fig. 3c, Fig. 4a) but magnetic field-independent (Fig 1c, Fig. 3d) TA and PL signal with 75-95% of the total emission (Fig. 3d). Thus, we observe the generation of the singlet states and strongly coupled ¹TT pairs, exhibiting a temperature-dependent decay via S* (assumed to be emissive the state in DPH systems, see section 4 in SI). The majority of PL arising during this period, and the absence of magnetic field dependence indicates that the weakly spin-correlated triplet pairs regime has not yet been reached.
2. **Regime II (40 - 100 ns):** In this intermediate regime, we begin to observe a magnetic field dependence in PL on the delayed fluorescence and in TA (Fig. 3d and 2c). EPR measurements (Fig. 2c) show that the quintet state, formed via weakly SCTP, already peaked within this time resolution. The TA signal is still decreasing through decaying ⁿTT states. This regime marks the onset of the weakly-coupled regime, which is also detectable already in the optical readout of MFE.
3. **Regime III (100 ns – approx. 2 μs):** This regime represents the completion of the strongly-coupled triplet pairs and the peak of the weakly-coupled regime. The MFE reaches its maximum, while the total PL achieves unity at 2 μs. Notably, the quintet signal in EPR diminishes by 2 μs, indicating that the remaining PL mainly originates from delayed ⁵TT states decaying via the optical back pathway, confirmed by only quintet ODMR signal at room temperature. The triplet signal in EPR peaks at approximately 800 ns, signifying the formation of SF-generated triplets, confirmed by the magnetic-field dependent splitting in TA in this time regime.
4. **Regime IV (until 300 μs):** This final regime features the decay of formed triplet states. The integrated PL no longer shows delayed emission, and the MFE is negligible. However, EPR still detects singlet fission-born triplet states, and TA measurements indicate a lifetime of these triplet states of around 300 μs.

Me-(DPH)₃ is distinguished from (DPH)₃ and (DPH)₂ by exclusively forming SF-generated triplets above 80 K, making it the only oligomer exhibiting the ideal pathways characteristic of an SF molecule. In contrast, (DPH)₃ in linear arrangement demonstrates an additional triplet generation pathway via ISC, which is, due to a one-to-one conversion, not beneficial for

optoelectronic energy devices. In contrast, (DPH)₂ lacks the capability to generate separated triplets, suggesting two directly linked chromophores being sufficient to generate weakly correlated triplet pairs but not for further separation.^{47,48} These results highlight that upon fast iSF to generate strongly exchange-coupled triplet pairs, the efficiency of dissociation into free triplets strongly depends on the overall geometry and the number of molecular units.

Furthermore, we studied the underexplored emission via quintet states in all oligomers. Pure quintet state formation in the strongly coupled regime, via mixing of SCTPs, is observed in all structures. These quintet states dominate the spin-dependent delayed emission and can be accessed at all temperatures above 30 K. Remarkably, emission via quintet states was observed by ODMR even at room temperature, a phenomenon never reported in the literature for iSF. This detailed spin-sensitive analysis provides a general framework for designing oligomers based on iSF for control and emission via high-spin states, suitable for various optoelectronic applications.

Methods

Transient absorption spectroscopy. Transient absorption experiments were conducted on a setup pumped by a Ti:sapphire amplifier (Solstice Ace, Spectra-Physics) emitting 200 fs pulses centred at 800 nm at a rate of 1 kHz and a total output of 7 W. The pump for sample excitation at 400 nm was provided by the second harmonic of the 800 nm output. To collect picosecond dynamics in the ultraviolet range, the output of the amplifier was used to seed a home-built broadband NOPA tuned to output 380–620 nm pulses generated by focusing the 800 nm fundamental beam onto a CaF₂ crystal (Eksma Optics, 5 mm) connected to a digital motion controller (Mercury C-863 DC Motor Controller), after passing through a mechanical delay stage. The transmitted pulses were collected with a single-line scan camera (JAI SW-4000M-PMCL) after passing through a spectrograph (Andor Shamrock SR-163).

For the nanosecond dynamics, the probe beam was generated with a supercontinuum laser (LEUKOS Disco 1 UV) and was delayed electronically with respect to the pump. The pump and probe beams were overlapped on the sample and focused into an imaging spectrometer (Andor, Shamrock SR 303i). The beams were detected using a pair of linear image sensors (Hamamatsu, G11608) driven and read out at the full laser repetition rate by a custom-built board from Stresing Entwicklungsbüro.

Electron paramagnetic resonance. Transient EPR (trEPR) was performed at a Bruker E580 EleXSys spectrometer using a Bruker ER4118-MD5-W1 dielectric TE01 δ mode resonator (around 9.70 GHz) in an Oxford Instruments CF935 cryostat. Pulsed optical excitation was performed with an Ekspla NT230 Laser with pulse length of 3 ns, and repetition rate of 50 Hz, using pulse energies of 1.0 mJ at 355 nm. Measurements have been performed with 25 dB attenuation (1.6 mW). By sweeping the magnetic field, two-dimensional data sets are recorded, where trEPR spectra are averaged at different time intervals after laser excitation. The amplifiers for pulsed EPR (Applied Systems Engineering) had saturated powers of 1.5 kW.

Optically detected magnetic resonance. ODMR experiments were carried out using a modified X-band spectrometer (Varian) equipped with a continuous-flow helium cryostat (Oxford Instruments CF935 cryostat) and a home-built optical resonator (based on Bruker ER4118-MD5-W1) with optical access. Optical irradiation was performed with a 365 nm LED (M365L3 Thorlabs) from one side-opening of the cavity. PL was detected with a silicon photodiode on the opposite opening, using a 375 nm long-pass filter to reject excitation light. The PL signal was amplified by a current/voltage amplifier (Femto DHPHA-200) and recorded by a lock-in detector (Stanford Research Systems SR830) referenced by on-off modulation of microwaves with a frequency of 517 Hz.

Transient photoluminescence. Transient PL spectra were collected using an electrically gated intensified CCD (ICCD) camera (Andor iStar DH740 CCI-010) coupled with an image identifier tube after passing through a calibrated grating spectrometer (Andor SR303i). Samples were excited using pump pulses obtained from a home-built narrowband NOPA whilst a suitable longpass filter (375 nm or 425 nm) avoided scattered laser signals entering the camera. The kinetics were obtained by setting the gate delay steps with respect to the excitation pulse. The gate widths of the ICCD were 4 ns, 10 ns, 250 ns, 1 μ s and 10 μ s, with overlapping time regions used to compose decays. Temperature-dependent measurements were performed using a closed-circuit pressurized helium cryostat (Optistat Dry BL4, Oxford Instruments), a compressor (HC-4E2, Sumitomo) and a temperature controller (Mercury iTC, Oxford Instruments).

Time-resolved magnetic field effect. Time-resolved MFE were performed with the similar electrically gated intensified CCD (Andor iStar DH334T-18U-73) camera as in trPL, whilst the excitation was performed by Q-switched Nd:YVO₄ laser (Piccolo AOT 1, Innolas) equipped

with integrated harmonic modules for frequency-tripling (to 355 nm) provided pump pulses (500 Hz, <800 ps nominal FWHM). The gate width of the ICCD was fixed for one time-resolved MFE trace at the given gate whilst the magnetic field was swept in 5-20mT steps. For magnetic field and temperature control, a magnetocryostat system (Montana He cryostat, 3.4-350K) with a Magneto-Optic module (cryostation s50 - MO) was used. Three measurements were taken at 0 mT as this is the reference measurement used to calculate the magnetic field effect.

Sample preparation. Solution samples were diluted in toluene (200 μ M). EPR and ODMR samples were prepared by multiple freeze-pump-thaw cycles in a EPR tube (3.9 mm OD). Thin film samples were prepared by molecules dispersed in polystyrene (0.1 wt%). For EPR and ODMR, multiple films were stacked in a EPR tube and flame-sealed under vacuum. Dilute solution and dispersed films were tested to give the same signals.

Acknowledgements

We acknowledge funding from the Physics of Sustainability and the Engineering Physical Sciences Research Council (U.K.) – EP/W017091/1 and EP/V055127/1. T.W.B. and J.C. acknowledge EPSRC for funding the cryomagnet and Lord Porter Laser Facility (EP/T012455/1, EP/L022613/1, EP/R042802/1) and EPSRC and Calico Life Sciences LLC for studentship support. W.K.M. acknowledges EPSRC (grant to CAESR, EP/L011972/1) & John Fell Fund (0007019 & 0010710). J.B. acknowledges financial support from the German Research Foundation (DFG grant number BE 5126/6-1).

Authors Contribution

J.G. performed the TA, EPR, ODMR and PL measurements. S.M. synthesized compounds. J.G. and T. W. B. performed the MFE measurements. S.D. prepared thin film samples. J.G. and N.C.G. designed experiments and analysed data. A.S., S.G. and O.M supported the data analysis. J.B., J.C., A.R., H.B. and N.C.G. supervised group members involved in the project. J.G. and N.C.G wrote the manuscript with input from all authors.

References

- 1 Smith, M. B. & Michl, J. Singlet fission. *Chem. Rev.* **110**, 6891-6936 (2010).
- 2 Smith, M. B. & Michl, J. Recent advances in singlet fission. *Annual review of physical chemistry* **64**, 361-386 (2013).
- 3 Baldo, M. A. *et al.* in *Electrophosphorescent Materials and Devices* 1-11 (Jenny Stanford Publishing, 2023).
- 4 Endo, A. *et al.* Thermally activated delayed fluorescence from Sn⁴⁺-porphyrin complexes and their application to organic light-emitting diodes-A novel mechanism for electroluminescence. *Adv. Mat.* **21**, 4802-4806 (2009).
- 5 Weiss, L. R. *et al.* Strongly exchange-coupled triplet pairs in an organic semiconductor. *Nat. Phys.* **13**, 176-181 (2017).
- 6 Tayebjee, M. J., McCamey, D. R. & Schmidt, T. W. Beyond Shockley–Queisser: molecular approaches to high-efficiency photovoltaics. *J. Phys. Chem. Lett.* **6**, 2367-2378 (2015).
- 7 Hanna, M. & Nozik, A. Solar conversion efficiency of photovoltaic and photoelectrolysis cells with carrier multiplication absorbers. *J. Appl. Phys.* **100** (2006).
- 8 Yamauchi, A. *et al.* Room-temperature quantum coherence of entangled multiexcitons in a metal-organic framework. *Sci. Adv.* **10**, eadi3147 (2024).
- 9 Jacobberger, R. M., Qiu, Y., Williams, M. L., Krzyaniak, M. D. & Wasielewski, M. R. Using molecular design to enhance the coherence time of quintet multiexcitons generated by singlet fission in single crystals. *J. Am. Chem. Soc.* **144**, 2276-2283 (2022).
- 10 Walker, B. J., Musser, A. J., Beljonne, D. & Friend, R. H. Singlet exciton fission in solution. *Nat. Chem.* **5**, 1019-1024 (2013).
- 11 Renaud, N. & Grozema, F. C. Intermolecular vibrational modes speed up singlet fission in perylenediimide crystals. *J. Phys. Chem. Lett.* **6**, 360-365 (2015).
- 12 Roberts, S. T. *et al.* Efficient singlet fission discovered in a disordered acene film. *J. Am. Chem. Soc.* **134**, 6388-6400 (2012).
- 13 Sanders, S. N. *et al.* Quantitative intramolecular singlet fission in bipentacenes. *J. Am. Chem. Soc.* **137**, 8965-8972 (2015).
- 14 Tayebjee, M. J. *et al.* Quintet multiexciton dynamics in singlet fission. *Nat. Phys.* **13**, 182-188 (2017).
- 15 Korovina, N. V. *et al.* Singlet fission in a covalently linked cofacial alkynyltetracene dimer. *J. Am. Chem. Soc.* **138**, 617-627 (2016).
- 16 MacDonald, T. S. *et al.* Anisotropic multiexciton quintet and triplet dynamics in singlet fission via pulsed electron spin resonance. *J. Am. Chem. Soc.* **145**, 15275-15283 (2023).
- 17 Kim, W. *et al.* Heterogeneous singlet fission in a covalently linked pentacene dimer. *Cell Rep. Phys. Sci.* **5**, 102045 (2023).
- 18 Korovina, N. V. *et al.* Linker-dependent singlet fission in tetracene dimers. *J. Am. Chem. Soc.* **140**, 10179-10190 (2018).
- 19 Burdett, J. J. & Bardeen, C. J. The dynamics of singlet fission in crystalline tetracene and covalent analogs. *Acc. Chem. Res.* **46**, 1312-1320 (2013).
- 20 Feng, X. & Krylov, A. I. On couplings and excimers: lessons from studies of singlet fission in covalently linked tetracene dimers. *Phys. Chem. Chem. Phys.* **18**, 7751-7761 (2016).

- 21 Korovina, N. V., Chang, C. H. & Johnson, J. C. Spatial separation of triplet excitons drives endothermic singlet fission. *Nat. Chem.* **12**, 391-398 (2020).
- 22 Wang, X. *et al.* Intramolecular singlet fission in a face-to-face stacked tetracene trimer. *Phys. Chem. Chem. Phys.* **20**, 6330-6336 (2018).
- 23 Millington, O. *et al.* *J. Am. Chem. Soc.* (2024).
<https://doi.org/10.1021/jacs.4c10483>
- 24 Japahuge, A. & Zeng, T. Theoretical studies of singlet fission: Searching for materials and exploring mechanisms. *ChemPlusChem* **83**, 146-182 (2018).
- 25 Burdett, J. J., Piland, G. B. & Bardeen, C. J. Magnetic field effects and the role of spin states in singlet fission. *Chem. Phys. Lett.* **585**, 1-10 (2013).
- 26 Musser, A. J. *et al.* The nature of singlet exciton fission in carotenoid aggregates. *J. Am. Chem. Soc.* **137**, 5130-5139 (2015).
- 27 Hashimoto, H., Uragami, C., Yukihiro, N., Gardiner, A. T. & Cogdell, R. J. Understanding/unravelling carotenoid excited singlet states. *J. R. Soc. Interface* **15**, 20180026 (2018).
- 28 Dillon, R. J., Piland, G. B. & Bardeen, C. J. Different rates of singlet fission in monoclinic versus orthorhombic crystal forms of diphenylhexatriene. *J. Am. Chem. Soc.* **135**, 17278-17281 (2013).
- 29 Lubert-Perquel, D. *et al.* Identifying triplet pathways in dilute pentacene films. *Nat. Comm.* **9**, 4222 (2018).
- 30 Millington, O. *et al.* Soluble diphenylhexatriene dimers for intramolecular singlet fission with high triplet energy. *J. Am. Chem. Soc.* **145**, 2499-2510 (2023).
- 31 Stoll, S. & Schweiger, A. EasySpin, a comprehensive software package for spectral simulation and analysis in EPR. *J. Magn. Reson.* **178**, 42-55 (2006).
- 32 Basel, B. S. *et al.* Unified model for singlet fission within a non-conjugated covalent pentacene dimer. *Nat. Comm.* **8**, 15171 (2017).
- 33 Richert, S., Tait, C. E. & Timmel, C. R. Delocalisation of photoexcited triplet states probed by transient EPR and hyperfine spectroscopy. *J. Magn. Reson.* **280**, 103-116 (2017).
- 34 Eaton, S. S., More, K. M., Sawant, B. M. & Eaton, G. R. Use of the ESR half-field transition to determine the interspin distance and the orientation of the interspin vector in systems with two unpaired electrons. *J. Am. Chem. Soc.* **105**, 6560-6567 (1983).
- 35 Gorgon, S. *et al.* Reversible spin-optical interface in luminescent organic radicals. *Nature* **620**, 538-544 (2023).
- 36 Grüne, J. *et al.* Triplet Excitons and Associated Efficiency-Limiting Pathways in Organic Solar Cell Blends Based on (Non-) Halogenated PBDB-T and Y-Series. *Adv. Funct. Mater.* **33**, 2212640 (2023).
- 37 Yago, T., Ishikawa, K., Katoh, R. & Wakasa, M. Magnetic field effects on triplet pair generated by singlet fission in an organic crystal: Application of radical pair model to triplet pair. *J. Phys. Chem. C* **120**, 27858-27870 (2016).
- 38 Wakasa, M. *et al.* What can be learned from magnetic field effects on singlet fission: Role of exchange interaction in excited triplet pairs. *J. Phys. Chem. C* **119**, 25840-25844 (2015).
- 39 Huang, Y. *et al.* Competition between triplet pair formation and excimer-like recombination controls singlet fission yield. *Cell Rep. Phys. Sci.* **2**, 100339 (2021).

- 40 Bayliss, S. L. *et al.* Spin signatures of exchange-coupled triplet pairs formed by singlet fission. *Phys. Rev. B* **94**, 045204 (2016).
- 41 Bossanyi, D. G. *et al.* Emissive spin-0 triplet-pairs are a direct product of triplet-triplet annihilation in pentacene single crystals and anthradithiophene films. *Nat. Chem.* **13**, 163-171 (2021).
- 42 Li, J., Chen, Z., Zhang, Q., Xiong, Z. & Zhang, Y. Temperature-dependent singlet exciton fission observed in amorphous rubrene films. *Org. Electron.* **26**, 213-217 (2015).
- 43 Kobori, Y., Fuki, M., Nakamura, S. & Hasobe, T. Geometries and Terahertz Motions Driving Quintet Multiexcitons and Ultimate Triplet-Triplet Dissociations via the Intramolecular Singlet Fissions. *J. Phys. Chem. B* **124**, 9411-9419 (2020).
- 44 Tsukushi, I. *et al.* Neutron scattering study of glassy toluene: dynamics of a quasi-rigid molecular glass. *J. Phys. Chem. Sol.* **60**, 1541-1543 (1999).
- 45 De Groot, H., De Jongh, L., Willett, R. & Reedijk, J. High-field (40 T) magnetization studies of linear Heisenberg chains with alternating exchange. *J. Appl. Phys.* **53**, 8038-8039 (1982).
- 46 Wolthuis, A., Huiskamp, W., De Jongh, L. & Reedijk, J. Magnetic and dielectric properties of copper methylpyridine halides. A dimerizing phase transition and random exchange behaviour. *Physica B+ C* **133**, 161-175 (1985).
- 47 Hetzer, C., Guldi, D. M. & Tykwinski, R. R. Pentacene dimers as a critical tool for the investigation of intramolecular singlet fission. *Chem. Eur. J.* **24**, 8245-8257 (2018).
- 48 Sakai, H. *et al.* Multiexciton dynamics depending on intramolecular orientations in pentacene dimers: Recombination and dissociation of correlated triplet pairs. *J. Phys. Chem. Lett.* **9**, 3354-3360 (2018).